UDC 620 . 186 . 5 : 539 . 4 . 072

Technical Report

Theoretical Analysis and Computer Simulation of Secondary Recrystallization in Grain-oriented Silicon Steel

Yoshiyuki USHIGAMI*

Abstract

The mechanism of secondary recrystallization in grain-oriented silicon steel has been studied on the basis of the statistical model of grain growth in which the inhibitor and texture are taken into account. The theoretical analysis reveals that this model explains the evolution of Goss-oriented grain to a coarse grain more than thousand times larger in diameter than the matrix grains by consuming a hundred million other grains. The computer simulation shows that this model successfully depicts the important features of secondary recrystallization; grain growth behavior of secondary grains, secondary grain size and sharpness of Goss texture.

1. Introduction

When steel is annealed at a higher temperature after the completion of primary recrystallization, specific grains in the primary recrystallized structure consume other grains in the structure and grow into coarse grains. This phenomenon is called secondary recrystallization. Grain-oriented silicon steel, which is used for transformer cores, is a typical industrial product in which secondary recrystallization is utilized to control grain orientation.

Grain-oriented silicon steel was invented by Goss in America in 1934.[1] Since then, extensive research and the development of steel has been carried out.[2-5] Today, it is one of Japan's high-performance steel products. Since the axis of the easy magnetization of iron is <001>[6], it is possible to improve the magnetic characteristics of iron by controlling its grain orientation. The average deviation angle from the <001> axis of the highest grade of existing products is approximately three degrees.

In stable secondary recrystallization, fine precipitates called inhibitors play an important role.[7-10] When primary recrystallized steel is annealed further, grains of all orientations grow. On the other hand, in the presence of an inhibitor, as shown in **Fig. 1**, the growth of grains is restrained by the pinning effect in the low-temperature region; however, at a temperature at which the inhibitor begins to weaken, only the {110}<001> grains or the Goss orientation starts growing into coarse grains.

In the secondary recrystallization of grain-oriented silicon steel, of the primary recrystallized grains having an average grain diameter of approximately 10 μm, only grains of the Goss orientation

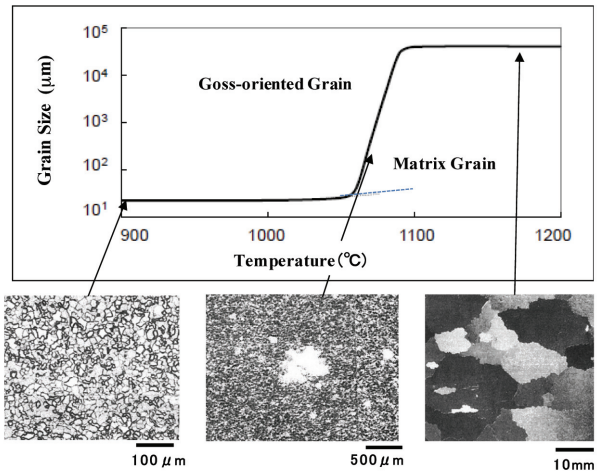

Fig. 1 Secondary recrystallization behavior in grain-oriented silicon steel (grain size and structure)

* Chief Researcher, Dr.Eng., Yawata R&D Lab.
1-1, Tobihata-cho, Tobata-ku, Kitakyushu, Fukuoka 804-8501

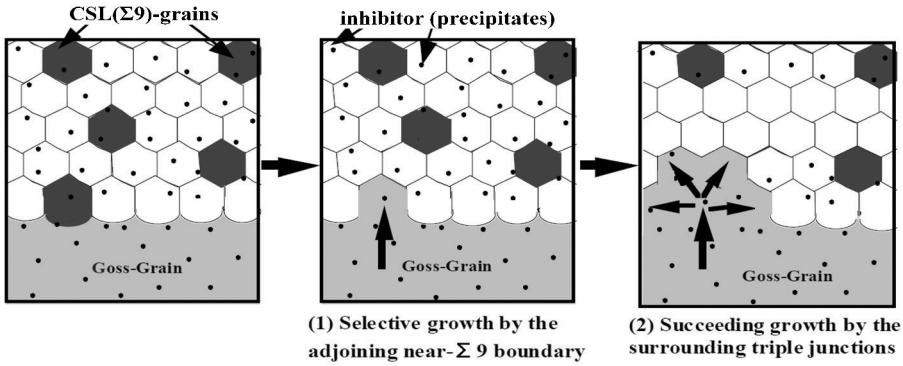

Fig. 2 CSL model of secondary recrystallization (elementary process of selective growth of Goss-oriented grain)[21, 22, 27]

grow into coarse grains more than 1,000 times larger (several to tens of mm). Grains of the Goss orientation grow by encroaching on as many as one hundred million other matrix grains. In the primary recrystallized structure, there is only about one grain of the Goss orientation per ten thousand matrix grains. Thus, only one out of approximately 10,000 × 10,000 primary recrystallized grains grows into a secondary recrystallized grain.

Many studies have reported the mechanism whereby only grains of the Goss orientation having a very low frequency grow preferentially.[11-16]

For clarifying the secondary recrystallization mechanism, we conducted a dynamic observation of secondary recrystallized grains using synchrotron radiation, which is a powerful X-ray source. On the basis of the observed results, we proposed a coincidence site lattice (CSL) model (**Fig. 2**)[17-22]. It is already known that Goss-oriented grains have a high frequency of coincidence grain boundaries, showing good lattice coherence with the surrounding matrix grains. Compared with the ordinary high-angle grain boundary, the coincidence grain boundary has lower grain boundary energy and is subject to a smaller pinning force from the inhibitor. This is considered to account for the preferential movement of the coincidence grain boundary. It is estimated that the macroscopic secondary recrystallization of Goss-oriented grains manifests itself with the above selective movement of the coincidence grain boundary under the presence of an inhibitor as a trigger.

In the present study, on the basis of the statistical grain growth theory, we (1) carried out a theoretical analysis to verify the mechanism whereby Goss-oriented grains grow into coarse grains more than 1,000 times larger, and then (2) compared the results of our computer simulation of secondary recrystallization with the actual behavior of secondary recrystallization.

2. Theoretical Study of Secondary Recrystallization

2.1 Theoretical analysis using the statistical grain growth model[23-27]

Generally, the growth of grains is classified as "continuous grain growth" and "discontinuous grain growth." **Fig. 3** schematically shows the behavior of continuous and discontinuous grain growth.[28] In continuous grain growth, the normalized grain size distribution itself remains the same, although the average grain size completely increases as small grains disappear (Fig. 3(a)). On the other hand, as shown in Fig. 3(b), discontinuous grain growth is the phenomenon whereby only specific grains grow to render the grain size distribution discontinuous when the growth of matrix grains is restrained by an inhibitor, etc.

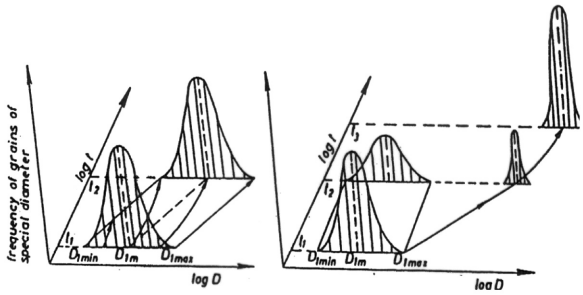

(a) Continuous grain growth (b) Discontinuous grain growth

Fig. 3 Schematics of continuous and discontinuous grain growth[28] (t: annealing time, D: grain diameter)

The term "secondary recrystallization" is sometimes used as a synonym for the term "discontinuous grain growth" explained above. However, when applied to grain-oriented silicon steel, secondary recrystallization has two salient characteristics: (1) only grains of a specific grain orientation (i.e., Goss-oriented grains) are involved in the phenomenon, and (2) those Goss-oriented grains grow into grains more than 1,000 times larger.

In the present study, we theoretically analyzed the above two characteristics using a statistical grain growth model. The model is schematically presented in **Fig. 4**. Based on a statistical model that assumes the driving force from matrix grains as the average field (E/R_c) from the same grain size,[29] our model considers the influences of inhibitor and texture (grain boundary energy). Using the model, we determined discontinuous grain growth by comparing the growth rate of Goss-oriented grains with that of matrix grains and verified the probability of Goss-oriented grains growing into coarse grains several thousand times larger.

The growth rate of Goss-oriented grains is expressed by the following equation.

$$\frac{dR_G}{dt} = AM\left(\frac{E}{R_C} - \frac{E_G}{R_G} - \frac{E_G I_Z}{A}\right), \quad (1)$$

where R_G: Goss-oriented grain radius, R_C: matrix grain critical radius, E_G: grain boundary energy between the Goss-oriented grain and matrix grains, E: grain boundary energy between matrix grains, t: time, A: form factor, M: grain boundary mobility, and I_Z: inhibitor strength.

As shown in Fig. 4 and Equation (1), three types of forces act on each Goss-oriented grain. The first term (P1) in Equation (1) is the driving force produced by the grain boundary tension of the matrix

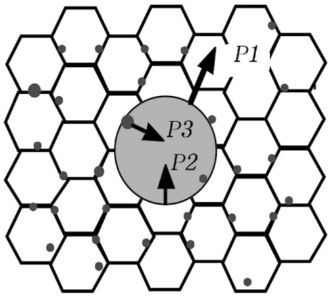

Fig. 4 Schematic illustration of microstructure and three forces that affect Goss-oriented grain[11, 27)]

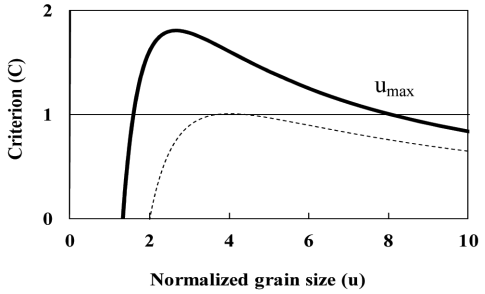

Fig. 5 Effect of grain boundary energy and inhibitor on criterion parameter of discontinuous grain growth (C)[27)] (dotted line: $z = 0.5,\ \Delta k_e = 0$, solid line: $z = 0.5,\ \Delta k_e = 0.2$)

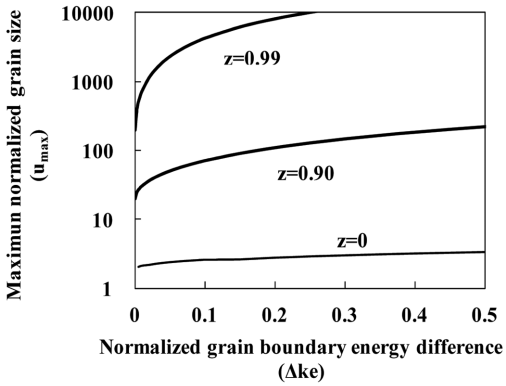

Fig. 6 Effect of grain boundary energy and inhibitor on maximum normalized grain size[24, 27)]

grain, and the second term (P2) is the self-shrinking force of the Goss-oriented grain. The third term (P3) is the inhibitor pinning force against the grain boundary movement. In the CSL model shown in Fig. 2, the third term ($E_G I_Z$) plays an important role.

In the manufacturing process of grain-oriented silicon steel, a primary recrystallized steel sheet wound as a coil is slowly heated up to approximately 1,200˚C over tens of hours to cause secondary recrystallization. In this heating process, matrix grains also grow as the pinning force of the inhibitor decreases. Therefore, it is considered that secondary recrystallization manifests itself in a quasi-steady state ($R_C I_Z$ = constant). The growth of matrix grains in the quasi-steady state is expressed by the following equation.[29)]

$$\frac{dR_c}{dt} = \frac{AME}{4R_c}\left(1 - \frac{R_c I_z}{A}\right)^2 \tag{2}$$

Whether discontinuous grain growth occurs can be judged using Equation (3) to obtain the ratio (C) of the relative growth rate of the Goss-oriented grain, expressed by Equation (1), to that of matrix grain expressed by Equation (2).

$$C = \left(\frac{dR}{R}\right) \Big/ \left(\frac{dR_c}{R_c}\right) \tag{3}$$

Discontinuous grain growth occurs when $C > 1$; that is, when the relative growth rate of the Goss-oriented grain is greater than that of the matrix grain. When we substitute Equations (1) and (2) for Equation (3) and express the grain size, the inhibitor, and grain boundary energy by the following normalized parameters (u, z, k_e), discontinuous grain growth can be calculated by the following equation.

$$u = \frac{R}{R_C},\ z = \frac{R_C I_Z}{A},\ k_e = \frac{E_G}{E}$$

$$C - 1 = -\frac{(1-z)^2 u^2 - 4(1 - k_e z)u + 4k_e}{(1-z)^2 u^2} \tag{4}$$

Fig. 5 shows an example in which we evaluated the influences of those parameters. It can be seen from the figure that the discontinuous growth of Goss-oriented grains does not occur ($C \leq 1$) when only the inhibitor is introduced ($z = 0.5,\ \Delta k_e = 1 - k_e = 0$), but that discontinuous grain growth occurs ($C > 1$) when not only the inhibitor but also the peculiarity of the grain boundary energy is introduced ($z = 0.5,\ \Delta k_e = 0.2$). As a result of discontinuous grain growth, the relative grain size increases. However, after the relative growth rate ratio (C) reaches its maximum, it starts to gradually decrease. Thus, it can be seen that when a certain maximum grain size (u_{max}) is reached, the grain cannot grow anymore.

Fig. 6 shows the influences of the inhibitor and grain boundary energy on the attainable maximum grain size (u_{max}). For discontinuous grain growth to occur, it is necessary that the grain boundary energy have a certain peculiarity ($\Delta k_e > 0$). However, to permit the grains to grow thousands of times larger, it is also necessary to increase the inhibitor strength. This requirement comes from the third term ($k_e I_z$) in Equation (1), suggesting that the coincidence grain boundary and inhibitor play an important role in secondary recrystallization.

The above analysis demonstrates that by introducing the inhibitor and grain boundary energy peculiarity in the statistical grain growth model, it is possible to explain that "Goss-oriented grains can grow into huge grains more than 1,000 times larger"—the salient characteristic of grain-oriented silicon steel.

2.2 Computer simulation of secondary recrystallization[30-32)]

This section describes the computer simulation we carried out to study to determine if it is possible to reproduce the behavior of secondary recrystallization.

2.2.1 Simulation model

Fig. 7 schematically shows the grain growth model used for the computer simulation. Generally, statistical grain growth can be expressed by the following equation.

$$\frac{dR_i^H}{dt} = \sum_K \sum_j \frac{S_j^K}{S} AM^{HK}\left(\frac{E^K}{R_j^K} - \frac{E^H}{R_i^H} - \frac{E^{HK} I_Z}{A}\right), \tag{5}$$

where R: grain radius, E: grain boundary energy, M: grain boundary mobility, t: time, S: grain boundary surface area, A: form factor, I_Z:

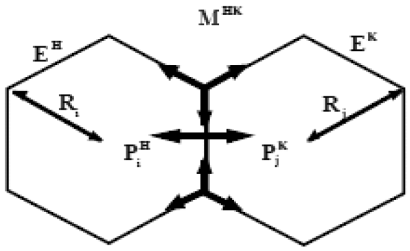

Fig. 7 Schematic illustration of the statistical model of grain growth for computer simulation[32)]

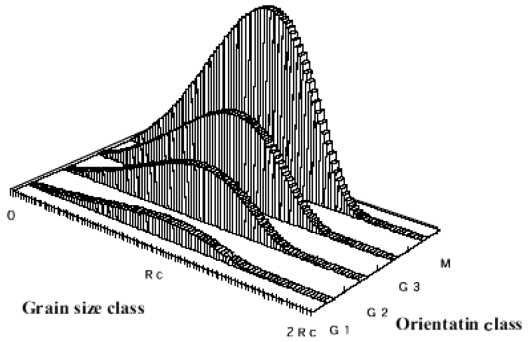

Orientation	M	G3	G2	G1
Frequency	0.9982	10×10^{-4}	6×10^{-4}	2×10^{-4}

Fig. 8 Initial conditions of grain structure (orientation and grain size distribution) and frequencies[32)]

inhibitor strength, (*H*, *K*): grain orientation class, and (*i*, *j*): grain size class.

Fig. 8 shows the initial state of a primary recrystallized structure. The grain orientations were divided into four classes: G1-G3 indicating the Goss orientations (dispersion angle: 5˚, 10˚, 15˚, respectively) and M indicating the matrix orientation. For the frequencies of the individual grain orientations, the results of our X-ray orientation distribution analysis of a sample prepared by a one-stage heavy cold-rolling process were used. The frequency of Goss-oriented grains is far lower than that of matrix grains. The initial grain size distribution was assumed to be of the 93 class, and Hillert's steady-state grain size distribution was used on the assumption that it would be unaffected by the grain orientation.[29)]

Grain boundaries were divided into three types, as shown in **Table 1**, and the relative grain boundary energy and relative grain boundary mobility shown in **Table 2** were used. As described in the preceding section, the difference in the grain boundary energy is considered to be the decisive factor. Therefore, in the present computer simulation, the peculiarity of mobility was not considered and mobility between the matrix grains was assumed to be similar to that between the Goss and matrix grains. In addition, with respect to the grain boundary energy of Goss grains and matrix grains, the grain boundary energy between Goss grains was assumed to be several percent (2%-4%) lower than that between matrix grains in view of the fact that the sharper the Goss-oriented grain, the greater the frequency of the coincidence grain boundary.

2.2.2 Comparative experiment[10)]

To verify our computer simulation, we carried out an experiment

Table 1 Characteristics of grain boundaries[32)]

Type of grain boundary	Energy	Mobility
Small angle boundary	Low	Low
High angle boundary	High	High
CSL boundary	Medium	Higher

Table 2 Relative grain boundary energy (e^{HK}) and relative grain boundary mobility (m^{HK}) between the orientation classes[32)]

e^{HK}	M	G3	G2	G1
M	1	0.98	0.97	0.96
G3	0.98	0.5	0.5	0.5
G2	0.97	0.5	0.5	0.5
G1	0.96	0.5	0.5	0.5

m^{HK}	M	G3	G2	G1
M	1	1	1	1
G3	1	0	0	0
G2	1	0	0	0
G1	1	0	0	0

on the influence of the inhibitor drop on the behavior of secondary recrystallization. In the experiment, secondary recrystallization annealing was performed isothermally, with the nitrogen partial pressure of the surrounding gas atmosphere varied to cause the decomposition behavior of the (Al, Si) N inhibitor to change so as to study the influence of the inhibitor on the behavior of secondary recrystallization.

As shown in **Fig. 9**, the secondary recrystallized structure and grain orientation distribution are markedly influenced by the rate of inhibitor drop. Thus, it can be confirmed that the inhibitor is an important governing factor. In the case of Specimen (a), when the nitrogen content of the atmosphere gas is increased to reduce the rate of inhibitor drop, only the sharp Goss-oriented grains grow preferentially, and the average size of secondary recrystallized grains becomes larger. Conversely, when the rate of inhibitor drop is increased, the dispersed Goss-oriented grains begin growing, and the average size of secondary recrystallized grains becomes small, and ultimately, the matrix grains also start growing as in Specimen (c).

2.2.3 Results of computer simulation[32)]

In the comparative experiment, we measured the amount and average size of inhibitor in each of the specimens with the rate of inhibitor drop varied and calculated the inhibitor strength. Using the experimental results, we carried out a computer simulation of the behavior of change in grain structures during secondary recrystallization annealing. In the simulation, a grain having a diameter greater or equal to twenty times that of the matrix grain was defined as a secondary recrystallized grain, and the time at which the volume fraction of the secondary recrystallized grains reached 1% and 99% was defined as the beginning and end, respectively, of secondary recrystallization.

Fig. 10 shows the experimental results (secondary recrystallized and matrix grain sizes) and the simulation results of the behavior of growth of Goss-oriented grains. According to the simulation results, when the nitrogen content of the atmosphere gas was increased to restrain the inhibitor drop, the secondary recrystallization beginning/ending times changed from 3.5 h/4.3 h to 5.0 h/5.9 h to 13.3 h/16.6 h. On the other hand, the ultimate average size of the secondary recrystallized grains increased from 3.4 mm to 7.8 mm to 26.8 mm. These simulation results reproduce the experimental results almost quantitatively. In addition, they reproduce the change in the secondary recrystallized grain size in the range from 100 to 1,000 times that of

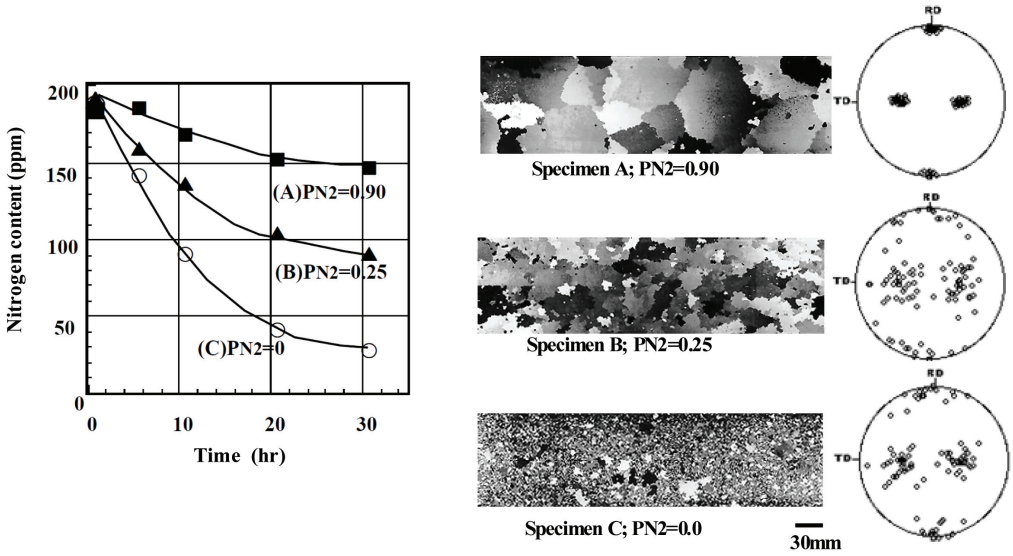

Fig. 9 Changes of nitrogen content during secondary recrystallization annealing (isothermal annealing at 1,075 °C) and grain structures and orientation distributions ({100} pole figures) after annealing[10, 32)]

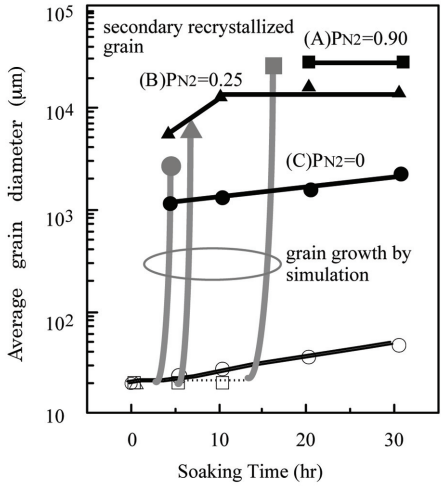

Fig. 10 Evolution of the average grain size of secondary grains and matrix grains during isothermal annealing (experimental and calculated values)[32)]

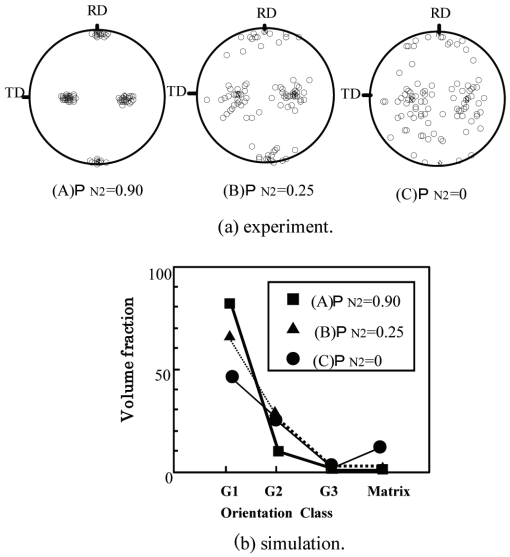

Fig. 11 Orientation distribution of secondary grains[32)]
(a) experiment ({100} pole figures), (b) simulation (volume fractions of four orientation classes)

the matrix grain size according to the rate of inhibitor drop.

Fig. 11 shows the results of the experiment and simulation of the secondary grain orientation distribution. According to the experimental results, when the rate of inhibitor increases, the dispersion of the Goss orientation gradually widens. In Specimen (c) with the highest rate of inhibitor drop, even grains other than Goss-oriented grains grow into coarse grains. The simulation results also show that with the increase in inhibitor drop rate, the volume fraction of G1—the sharp Goss-orientation class—decreases gradually, and the volume fractions of G2 and G3—the dispersed Goss-orientation classes—increase. In Specimen (c) with the highest rate of inhibitor drop, matrix grains (M) and Goss grains (G1-G3) become coarse and mix in the secondary recrystallized structure. These results agree with the experimental results.

As has been described above, by our computer simulation using the statistical grain growth model, we quantitatively reproduced the growth behavior of Goss-oriented grains into huge grains approximately 1,000 times larger and the grain size and grain orientation distribution.

3. Conclusions[33, 34)]

On the basis of the statistical grain growth theory, we studied the mechanisms of secondary recrystallization. Using the coincidence site lattice (CSL) model, which assumes that “coincidence grain boundaries having good lattice coherence move about preferentially because they are subject to a smaller pinning force from the inhibitor

than ordinary high-angle grain boundaries," we formulated the secondary recrystallization phenomenon of Goss-oriented grains. As a result of our theoretical analysis of secondary recrystallization using the equations of grain growth, it was possible to explain that "each Goss-oriented grain consumes as many as a hundred million matrix grains to become a huge grain more than 1,000 times larger in size." In addition, we showed that the computer simulation permits the quantitative reproduction of the growth behavior of Goss-oriented grains, such as the secondary recrystallization beginning/ending time, and the characteristics of secondary recrystallization, such as the secondary recrystallized grain size and the secondary recrystallized orientation distribution.

By utilizing the theory of secondary recrystallization mechanisms and the computer simulation technique that have been described, it is considered possible to further improve the advantageous characteristics of grain-oriented silicon steel.

References

1) Goss, N. P.: U.S.P. 1965559, 1934
2) Littmann, M. F., Heck, J. E.: U.S.P. 2599340, 1952
3) Taguchi, S., Sakakura, A.: Japanese Pat. Sho 33-4710. 1958
4) Goto, I., Matoba, I., Imanaka, T., Gotoh, T., Kan, T.: Proc. Soft Mag. Mat. 2, 262 (1975)
5) Takahashi, N., Suga, Y., Kobayashi, H.: J. Mag. Mag. Mat. 160, 143 (1996)
6) Honda, K., Kaya, S.: Sci. Repts. Tohoku Univ. 15, 721 (1926)
7) May, J. E., Turnbull, D.: Trans. Met. Soc. AIME. 212, 769 (1958)
8) Matsuoka, T.: Tetsu-to-Hagané. 53, 1007 (1967)
9) Ushigami, Y., Nakayama, T., Suga, Y., Takahashi, N.: Materials Science Forum. 204-206, 599 (1996)
10) Ushigami, Y., Murakami, K., Kubota, T.: Proc. 4th Int. Conf. on Recrystallization and Related Phenomena. 1999, p. 559
11) Matsuo, M., Sakai, T., Tanino, M., Shindo, T., Hayami, S.: Proc. 6th Int. Conf. on Textures of Materials, 1982, p. 918
12) Inokuti, Y., Maeda, C., Ito, Y., Shimanaka, H.: Proc. 6th Int. Conf. on Textures of Materials. 1982, p. 948
13) Harase, J., Shimizu, R., Dingley, D. J.: Acta Metall. 39, 763 (1991)
14) Hutchinson, B., Homma, H.: Proc. 3rd Int. Conf. on Grain Growth, 1998, p. 387
15) Hayakawa, Y., Szpunar, J. A.: Acta Mater. 45, 1285 (1997)
16) Park, H., Kim, D., Hwang, N., Joo, Y., Han, C. H., Kim, J.: J. Appl. Phys. 95, 5515 (2004)
17) Ushigami, Y., Suga, Y., Takahashi, N., Kawasaki, K., Chikaura, Y., Kii, H.: J. Mater. Eng. 13, 113 (1991)
18) Ushigami, Y., Kawasaki, K., Nakayama, T., Suga, Y., Harase, J., Takahashi, N.: Materials Science Forum. 157-162, 1081 (1994)
19) Ushigami, Y., Murakami, K., Kubota, T.: Proc. 3rd Int. Conf. on Grain Growth. 1998, p. 491
20) Ushigami, Y., Kubota, T., Takahashi, N.: Textures and Microstructures. 32, 137 (1999)
21) Ushigami, Y., Kumano, T., Haratani, T., Nakamura, S., Takebayashi, S., Kubota, T.: Mater. Sci. Forum. 467-470, 853 (2004)
22) Ushigami, Y., Nakamura, S., Takebayashi, S.: Heat Treatment. 50, 179 (2010)
23) Nakayama, T., Ushigami, Y.: Proc. 7th RISO Int. Symp. Met. Mat. Sci. 1986, p. 463
24) Ushigami, Y.: CAMP-ISIJ. 21, 548 (2008)
25) Ushigami, Y.: CAMP-ISIJ. 22, 1438 (2008)
26) Ushigami, Y., Nakamura, S., Fujikura, M.: CAMP-ISIJ. 26, 1231 (2010)
27) Ushigami, Y., Nakamura, S.: Materials Science Forum. 715-716, 122 (2012)
28) Detert, K.: Recrystallization of Metallic Materials. Ed. Haessner, F., 1978, p. 99
29) Hillert, M.: Acta Metall. 13, 227 (1965)
30) Nakayama, T., Ushigami, Y.: Materials Science Forum. 94-96, 413 (1992)
31) Nakayama, T., Ushigami, Y., Nagashima, T., Suga, Y., Takahashi, N.: Materials Science Forum. 204-206, 611 (1996)
32) Ushigami, Y., Nakayama, T., Arai, S., Kubota, T.: Proc. Soft Mag. Mater. 16, 2003, p. 487
33) Ushigami, Y.: Recrystallization/Textures and Their Application to Structural Control. The Iron and Steel Institute of Japan, 1999, p. 245
34) Ushigami, Y.: Japan Institute of Metals Seminar "An Attempt to Interpret the Riddle of Textures." 2001, p. 63

Yoshiyuki USHIGAMI
Chief Researcher, Dr.Eng.
Yawata R&D Lab.
1-1, Tobihata-cho, Tobata-ku, Kitakyushu,
Fukuoka 804-8501